Recipe for preparing a molecular ensemble with macroscopic threefold symmetry

Hiroto Nakabayashi,[1,*] Wataru Komatsubara,[1] and Hirofumi Sakai[1,2,†]

[1]*Department of Physics, Graduate School of Science, The University of Tokyo, 7-3-1 Hongo, Bunkyo-ku, Tokyo 113-0033, Japan*

[2]*Institute for Photon Science and Technology, Graduate School of Science, The University of Tokyo, 7-3-1 Hongo, Bunkyo-ku, Tokyo 113-0033, Japan*

(Received 16 November 2018; published 23 April 2019)

We propose how to prepare a molecular ensemble with macroscopic threefold symmetry. By utilizing the special laser electric field trajectory with threefold symmetry, which can be formed by superposing a counterrotating circularly polarized fundamental pulse and its second harmonic pulse, sample molecules with threefold symmetry such as BX_3 (X = F, Cl, Br, I) can be aligned with their three arms along (or in between) the laser electric fields with threefold symmetry depending on the sign of the hyperpolarizability of the sample molecule. We show that this method is feasible with practical experimental conditions as for the rotational temperature of the sample molecules and the intensities of the two wavelengths. This method will open up physics of symmetry concerning a molecular ensemble with macroscopic threefold symmetry.

DOI: 10.1103/PhysRevA.99.043420

The spatial control of gaseous molecules is one of the hot topics in molecular science over the last two decades. When it comes to the spatial control of gaseous molecules, researchers usually call molecular alignment and/or orientation to mind. When molecules are aligned, the molecular axes are parallel to each other with the equal distribution of the head-versus-tail order. On the other hand, when molecules are oriented, more than half of the sample molecules are directed the same direction. A sample of aligned or oriented molecules is an ideal anisotropic quantum system for many applications, which include stereodynamics of chemical reactions [1], electronic stereodynamics in molecules [2], shooting molecular movies with x-ray free-electron laser pulses [3–5], a quantum computation [6], and the selective preparation of one of the enantiomers from the 50:50 racemate [7]. The modern molecular alignment and orientation techniques are based on laser technologies. Since the pioneering works demonstrating the first adiabatic molecular alignment with an intense nonresonant laser field [8,9], the molecular alignment techniques have been well developed and utilized in various applications [10].

Among many proposals for achieving molecular orientation, first developed were the techniques with combined weak electrostatic and intense nonresonant laser fields (the combined-field technique) [11,12]. Both one- [13,14] and three-dimensional orientation [15] of ordinary molecules were demonstrated by our group. Then laser-field-free molecular orientation was achieved by rapidly turning off the nanosecond laser pulse with the plasma shutter technique [16,17]. Furthermore, by utilizing the advantage of state-selected sample molecules [18,19], laser-field-free one- [20] and three-dimensional molecular orientations [21] were achieved. The latter is the most advanced molecular orientation technique based on the combined-field technique because all the requirements (laser-field-free condition, three-dimensional control, and higher degrees of orientation) desired for the molecular orientation technique are achieved.

Another molecular orientation technique is based on the hyperpolarizability interaction between the induced dipole of the molecule and an intense nonresonant two-color laser field [22]. This all-optical molecular orientation was demonstrated with intense nonresonant nanosecond laser pulses [23]. The advantage of using nanosecond laser pulses is that field-free three-dimensional molecular orientation will be achieved by rapidly turning off the nanosecond two-color pulses with crossed polarizations [24]. In addition, the field-free molecular orientation with an intense femtosecond two-color laser field is also reported [25–27].

The all-optical technique with an intense nonresonant two-color laser field can be utilized to prepare a totally new class of molecular ensemble. In this article, we show how to prepare a new class of molecular ensemble with macroscopic threefold symmetry. By superposing a counterrotating circularly polarized fundamental (ω) pulse and its second harmonic (2ω) pulse, the special laser electric field trajectory with threefold symmetry is formed. The shape of the laser electric field trajectory depends on the ratio of the electric field strength ($\mathcal{E}_\omega$) of the fundamental pulse to that ($\mathcal{E}_{2\omega}$) of its second harmonic pulse as shown in Fig. 1. Through the hyperpolarizability interaction of the sample molecules such as BX_3 (X = F, Cl, Br, I) with threefold symmetry, a molecular ensemble with macroscopic threefold symmetry can be prepared with their three arms along (or in between) the laser electric fields with threefold symmetry. The feasibility of this technique is confirmed for practical experimental conditions concerning the rotational temperatures of the sample molecules and the intensities of the two wavelengths.

*0086531810@edu.k.u-tokyo.ac.jp
†hsakai@phys.s.u-tokyo.ac.jp

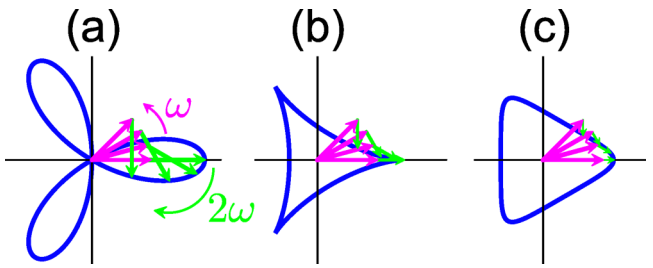

FIG. 1. The laser electric field trajectory with threefold symmetry is formed by superposing a counterrotating circularly polarized fundamental (ω) pulse and its second harmonic (2ω) pulse. The ratios of the electric field strength ($\mathcal{E}_\omega$) of the fundamental pulse to that ($\mathcal{E}_{2\omega}$) of its second harmonic pulse are (a) 1:1, (b) 2:1, and (c) 4:1.

First we define the laboratory-fixed coordinate system as (x, y, z) and the body-fixed coordinate system as (X, Y, Z), respectively. The laser electric field with an angular frequency ω propagating along the z axis is expressed as

$$\begin{aligned}\mathcal{E}(\omega) &= \mathcal{E}_L(\omega)e^{i\omega t} + \mathcal{E}_R(\omega)e^{-i\omega t} \\ &= \mathcal{E}(\omega)(z_L e^{i\omega t} + z_R e^{-i\omega t}),\end{aligned} \tag{1}$$

where $|z_L(\omega)|^2 + |z_R(\omega)|^2 = 1$. Then the laser electric field formed by superposing a counterrotating circularly polarized fundamental (ω) pulse and its second harmonic (2ω) pulse is given by

$$\mathcal{E} = \mathcal{E}(\omega) + \mathcal{E}(2\omega). \tag{2}$$

In Eq. (1), $z_C(\omega) = z_C$, $z_C(2\omega) = \zeta_C$, $(C = L, R)$ and $\mathcal{E}(\omega) = \mathcal{E}_1$ and $\mathcal{E}(2\omega) = \mathcal{E}_2$. Here the relative phase between the two wavelengths is assumed to be zero. We consider sample molecules with threefold symmetry such as BX_3 (X = F, Cl, Br, I), $C_6H_3X_3$ (X = F, Cl, Br, I), $Fe(CO)_5$ (pentacarbonyl iron), $N_3B_3H_6$ (borazine), and so on. These molecules belong to the point group D_{3h} and are assumed to be rigid. The Hamiltonian is given by

$$\begin{aligned}H(t) = &\frac{J_X^2 + J_Y^2}{2I_X} + \frac{J_Z^2}{2I_Z} \\ &+ \frac{-\alpha_{20}}{4}\left[(\mathcal{E}^*)^2\mathcal{D}^{(2)}_{02} - \sqrt{\frac{2}{3}}\mathcal{E}\mathcal{E}^*\mathcal{D}^{(2)}_{00} + \mathcal{E}^2\mathcal{D}^{(2)}_{0-2}\right] + \sqrt{\frac{1}{12}}\alpha_{00}\mathcal{E}\mathcal{E}^* \\ &+ \frac{\beta_\Delta}{24}\left[(\mathcal{E}^*)^3\left(\mathcal{D}^{(3)}_{33} - \mathcal{D}^{(3)}_{-33}\right) - \sqrt{\frac{3}{5}}(\mathcal{E}^*)^2\mathcal{E}\left(\mathcal{D}^{(3)}_{31} - \mathcal{D}^{(3)}_{-31}\right) + \sqrt{\frac{3}{5}}\mathcal{E}^*\mathcal{E}^2\left(\mathcal{D}^{(3)}_{3-1} - \mathcal{D}^{(3)}_{-3-1}\right) - \mathcal{E}^3\left(\mathcal{D}^{(3)}_{3-3} - \mathcal{D}^{(3)}_{-3-3}\right)\right],\end{aligned} \tag{3}$$

where J_K $(K = X, Y, Z)$ is the angular momentum in the body-fixed coordinate system in units of $\hbar$, I_K is the moment of inertia along the axis K, α_{ij} is a linear polarizability, $\beta_\Delta = -2\beta_{XXX} = 2\beta_{XYY} = 2\beta_{YXY} = 2\beta_{YYX}$ is the hyperpolarizability, and $\mathcal{D}^{(j)}_{km}$ is the Wigner D-matrix [28]. The Hamiltonian includes three kinds of contributions: the first line of the right-hand side of Eq. (3) is the energy of the free rotation of a symmetric top, the second line is the polarizability interaction potential (the interaction potential between the laser electric field and the linear polarization), and the third line is the hyperpolarizability interaction potential (the interaction potential between the laser electric field and the second-order nonlinear polarization). In this study, we assume that the interaction is adiabatic and we solve the time-independent Schrödinger equation.

In order to characterize how well the sample molecules are aligned in the counterrotating circularly polarized two-color laser field with their three arms along (or in between) the laser electric fields with threefold symmetry, we propose the order parameter

$$\begin{aligned}I_\Delta &= \frac{1}{3}\sum_{i=0}^{2} r_i^3 \cos 3\phi_i \\ &= \frac{1}{2}\left(\mathcal{D}^{(3)}_{33} - \mathcal{D}^{(3)}_{3-3} - \mathcal{D}^{(3)}_{-33} + \mathcal{D}^{(3)}_{-3-3}\right),\end{aligned} \tag{4}$$

where r_i is the normalized arm length of the sample molecule projected to the circular polarization plane of the two-color laser pulse and ϕ_i is the azimuthal angle. The order parameter I_Δ ranges from -1 to 1. As shown in Fig. 2, one can see that the order parameter $|I_\Delta|$ becomes larger as the sample molecules are better aligned in the counterrotating circularly polarized two-color laser field with their three arms along (or in between) the laser electric fields with threefold symmetry. For the thermal ensemble at the rotational temperature T, we consider the ensemble average of I_Δ, $\langle I_\Delta\rangle$, which is given by

$$\langle I_\Delta\rangle = \frac{\sum_n e^{-E_n/k_BT}\langle E_n|I_\Delta|E_n\rangle}{\sum_n e^{-E_n/k_BT}}, \tag{5}$$

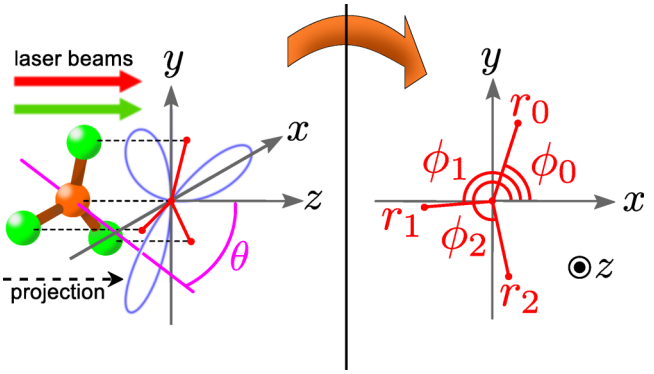

FIG. 2. Illustration of the physical meaning of the order parameter $\langle I_\Delta\rangle$. When the sample molecule is better aligned in the counterrotating circularly polarized two-color laser field with their three arms along (or in between) the laser electric fields with threefold symmetry, the order parameter $|\langle I_\Delta\rangle|$ takes a larger value.

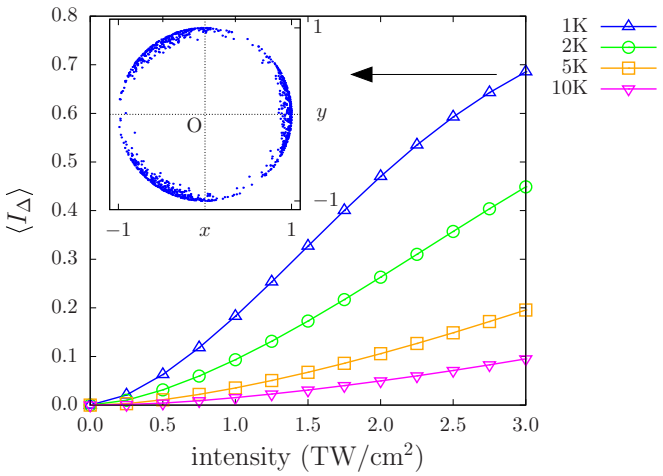

FIG. 3. The order parameter $\langle I_\Delta \rangle$ as a function of the intensity of each wavelength for different rotational temperatures. The inset shows the angular distribution of sample molecules projected onto the x-y plane achieved at both the intensities of the two wavelengths of 3.0×10^{12} W/cm^2 and for the rotational temperature of 1 K, when $\langle I_\Delta \rangle = 0.69$ is achieved [31].

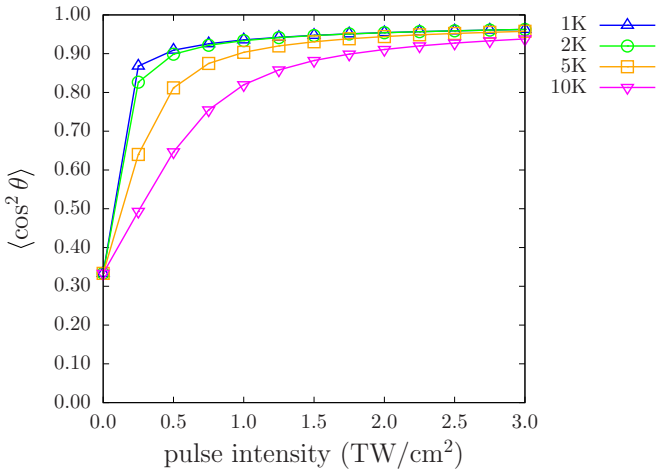

FIG. 4. The $\langle \cos^2 \theta \rangle$ as a function of the intensity of each wavelength for different rotational temperatures. Note that $\langle \cos^2 \theta \rangle = 1/3$ for the randomly oriented sample molecules.

where E_n is the eigenvalue for the Hamiltonian [Eq. (3)] with the cycle-averaged electric field of the two wavelengths [Eqs. (1) and (2)] and k_B is the Boltzmann constant.

Here we consider a model molecule because there are no specific molecules whose all molecular constants necessary for the numerical simulations are known. For the model molecule, we assume the following constants: $A/hc = B/hc = 0.2$ cm^{-1}, $C/hc = 0.01$ cm^{-1}, $\alpha_{XX} = \alpha_{YY} = 80$ a.u., $\alpha_{ZZ} = 50$ a.u., and $\beta_\Delta = -100$ a.u. The rotational constants are the representative values of the planar molecules. The contribution of the free rotation of the rigid sample molecule to the eigenenergy is very small compared to those from the polarizability interaction and the hyperpolarizability interaction with the laser electric field, producing very little effect on the order parameter I_Δ. The polarizability components are the averaged values of those of the BX_3 (X = F, Cl, Br, I) molecules, which are reported in Ref. [29]. The hyperpolarizability is determined based on the following considerations [30]: A typical electric field which an electron in the sample molecule feels is the Coulombic field formed by the nucleus, which is on the order of $E_0 = E_\mathrm{h}/ea_0$ with E_h the Hartree energy, e the elementary charge, and a_0 the Bohr radius. When the induced dipole is expanded by the power of the dimensionless parameter E/E_0, the relationship between the polarizability α and the hyperpolarizability β is expected to be $\alpha \sim E_0\beta$. The sign of β is determined by the definition of the coordinate X and has no influence on the magnitude of the order parameter $|I_\Delta|$. One can see that the polarizability components and the hyperpolarizability of the model molecule thus estimated are reasonable when compared to those of the linear molecule.

Assuming that the intensity ratio of the two wavelengths is 1:1 as shown in Fig. 1(a), Fig. 3 shows the $\langle I_\Delta \rangle$ as a function of the intensity of each wavelength for different rotational temperatures. The rotational temperature lower than 10 K can be achieved by the pulsed molecular beam technique. One can see that both the lower rotational temperature and the higher laser intensity are of crucial importance to achieve higher order parameters. For the rotational temperature lower than 10 K, the order parameter $\langle I_\Delta \rangle > 0.1$ can be achieved at 3.0×10^{12} W/cm^2 for the intensity of each wavelength. The order parameter $\langle I_\Delta \rangle > 0.4$ can be achieved for the rotational temperature lower than 2 K. The inset of Fig. 3 shows the angular distribution of sample molecules projected onto the x–y plane achieved at both the intensities of the two wavelengths of 3.0×10^{12} W/cm^2 and for the rotational temperature of 1 K, when $\langle I_\Delta \rangle = 0.69$ is achieved [31]. The fact that higher order parameters can be achieved at lower rotational temperature means that even higher order parameters could be achieved by using sample molecules in lower-lying rotational states [18–21]. Since the results shown in Fig. 3 show no saturation tendency at 3.0×10^{12} W/cm^2 for the intensity of each wavelength, one can expect higher order parameters at higher intensities of each wavelength as long as the ionization of the sample molecules is not significant.

We also examine how the planes of the sample molecules are well aligned along the plane of the laser polarization with threefold symmetry, which is characterized by $\langle \cos^2 \theta \rangle$ with the polar angle θ as shown in Fig. 2. Figure 4 shows $\langle \cos^2 \theta \rangle$ as a function of the intensity of each wavelength for different rotational temperatures. In sharp contrast to the intensity dependence of the order parameter $\langle I_\Delta \rangle$, $\langle \cos^2 \theta \rangle$ increases rapidly at lower intensities of each wavelength and shows strong saturation tendency at the intensity higher than 2.5×10^{11}, 5.0×10^{11}, and 1.0×10^{12} W/cm^2 for the rotational temperatures of 1–2 K, 5 K, and 10 K, respectively. In addition, $\langle \cos^2 \theta \rangle$ is insensitive to the rotational temperature below ~5 K.

Figure 5 shows the $\langle I_\Delta \rangle$ as a function of the polarization state of the second harmonic pulse, which is defined by $\tan \eta$ with $\zeta_R = \cos \eta$ and $\zeta_L = \sin \eta$, and the horizontal axis is given by the angle η (degrees). The polarization of the fundamental pulse is left circularly polarized. Both the intensities of the fundamental pulse and its second harmonic pulse are assumed to be 3.0×10^{12} W/cm^2. When $\eta = 0$ degrees, which corresponds to the right circularly polarized 2ω pulse, the order parameter $\langle I_\Delta \rangle$ takes the highest value (0.69 for 1 K) as expected. The order parameter $\langle I_\Delta \rangle$ decreases as the

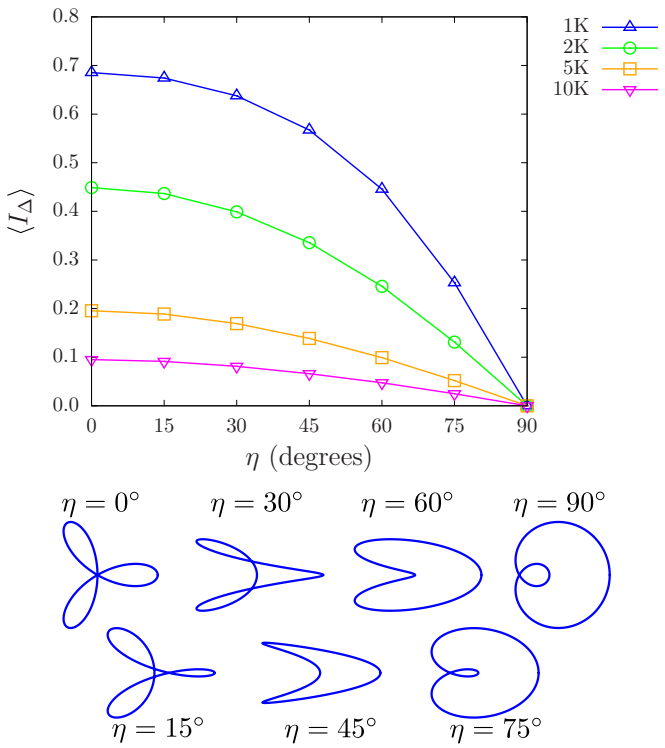

FIG. 5. The order parameter as a function of the polarization state of the second harmonic pulse, which is defined by $\tan\eta$ with $\zeta_R = \cos\eta$ and $\zeta_L = \sin\eta$, and the horizontal axis is given by the angle η (degrees). The polarization of the fundamental pulse is left circularly polarized. Both the intensities of the fundamental pulse and its second harmonic pulse are assumed to be 3.0×10^{12} W/cm^2. The laser electric field trajectories for $\eta = 0°$, $15°$, $30°$, $45°$, $60°$, $75°$, and $90°$ are illustrated in the lower part.

angle η increases. When $\eta = 45$ degrees, which corresponds to the linearly polarized 2ω pulse, the $\langle I_\Delta \rangle$ is still relatively high (0.57 for 1 K) because the superposed two-color laser electric field still has a boomerang-shaped trajectory with three projecting parts as illustrated in the lower part of Fig. 5. Then when $\eta = 90$ degrees, which corresponds to the left circularly polarized 2ω pulse and the electric fields of both ω and 2ω pulses rotate in the same direction, the $\langle I_\Delta \rangle$ becomes zero because of the disappearance of the threefold symmetry of the superposed two-color laser electric field.

The preparation of a molecular ensemble with macroscopic threefold symmetry could be confirmed by observing the angular distributions of the fragment ions produced with circularly polarized femtosecond probe pulses. To observe those fragment ions produced in the circular polarization plane of the two-color pump pulse, they are to be first extracted by utilizing the ion optics technique and then to be projected onto the two-dimensional ion detector [32]. The ion images on the detector plane are recorded by a CCD camera.

We make a brief comment on the possible extension of the present basic concept to the preparation of a molecular ensemble with macroscopic n-fold symmetry ($n \geqslant 4$). As in a molecular ensemble with macroscopic threefold symmetry, the interaction between the sample molecules with n-fold symmetry and the laser electric field with n-fold symmetry formed by superposing the counterrotating fundamental pulse and its $(n-1)$th-harmonic pulse theoretically leads to the preparation of a molecular ensemble with macroscopic n-fold symmetry through the $(n-2)$th hyperpolarizability interaction. Although the $(n-2)$th hyperpolarizability interaction is generally weaker than the $(n-3)$th hyperpolarizability interaction typically by two orders of magnitudes, it may be enhanced by the assistance of the interaction between the n-pole moment induced in the sample molecule and an n-pole electrostatic field or an n-pole magnetic field as in the combined-field technique for molecular orientation [17,18]. We hope that the present recipe triggers the future extension to the preparation of a molecular ensemble with macroscopic n-fold symmetry ($n \geqslant 4$).

In summary, we show that a molecular ensemble with macroscopic threefold symmetry can be prepared by exposing the sample molecules with threefold symmetry to a special laser electric field with threefold symmetry, which can be formed by superposing a counterrotating circularly polarized fundamental pulse and its second harmonic pulse. Then the sample molecules are aligned with their three arms along (or in between) the laser electric fields with threefold symmetry depending on the sign of the hyperpolarizability of the sample molecule. The feasibility of this technique is confirmed for practical experimental conditions as for the rotational temperature of the sample molecules and the intensities of the two wavelengths. A molecular ensemble with macroscopic threefold symmetry will be prepared even in the field-free condition by rapidly turning off the laser electric field with threefold symmetry with the plasma shutter technique [17,20,21].

This study will surely trigger future developments of various techniques for preparing molecular ensembles with macroscopic n-fold symmetry, opening up physics of symmetry concerning a molecular ensemble with macroscopic n-fold symmetry from an experimental point of view. Recently, researchers working in the fields of high-intensity laser physics, ultrafast phenomena, and molecular science have been very much interested in the selection rules of high-order harmonic generation from a molecular ensemble with macroscopic n-fold symmetry [33]. For example, in the case of a molecular ensemble with macroscopic threefold symmetry, the theory predicts that the $(3k \pm 1)$th harmonics are generated with a circularly polarized driving pulse and the $(k \pm 1)$th harmonics are generated with a linearly polarized driving pulse [33]. Although there had been no experimental methods to prepare a molecular ensemble with macroscopic n-fold symmetry, the present technique will allow us to verify the theoretical predictions experimentally. Furthermore, preparing a molecular ensemble with macroscopic n-fold symmetry means that a new class of molecular ensembles can be used in various applications including electronic stereodynamics in molecules [2] as well as stereodynamics of chemical reactions [1].

This project is supported by MATSUO FOUNDATION. The authors thank Prof. Akira Yagishita (Inter-University Research Institute Corporation, High-Energy Accelerator Research Organization) for his continued encouragement and support. W.K. is grateful for the financial support from the Advanced Leading Graduate Course for Photon Science (ALPS) of Ministry of Education, Culture, Sports, Science, and Technology.

[1] Eur. Phys. J. D **38**, No. 1 (2006), special issue on Stereodynamics of Chemical Reactions.

[2] D. Herschbach, Eur. Phys. J. D **38**, 3 (2006).

[3] J. Küpper *et al.*, Phys. Rev. Lett. **112**, 083002 (2014).

[4] K. Nakajima, T. Teramoto, H. Akagi, T. Fujikawa, T. Majima, S. Minemoto, K. Ogawa, H. Sakai, T. Togashi, K. Tono, S. Tsuru, K. Wada, M. Yabashi, and Y. Akira, Sci. Rep. **5**, 14065 (2015).

[5] S. Minemoto, T. Teramoto, H. Akagi, T. Fujikawa, T. Majima, K. Nakajima, K. Niki, S. Owada, H. Sakai, T. Togashi, K. Tono, S. Tsuru, K. Wada, M. Yabashi, S. Yoshida, and A. Yagishita, Sci. Rep. **6**, 38654 (2016).

[6] E. Shapiro, I. Khavkine, M. Spanner, and M. Y. Ivanov, Phys. Rev. A **67**, 013406 (2003).

[7] Y. Fujimura, L. González, K. Hoki, J. Manz, and Y. Ohtsuki, Chem. Phys. Lett. **306**, 1 (1999).

[8] H. Sakai, C. Safvan, J. J. Larsen, K. M. Hilligsøe, K. Hald, and H. Stapelfeldt, J. Chem. Phys. **110**, 10235 (1999).

[9] J. J. Larsen, H. Sakai, C. Safvan, I. Wendt-Larsen, and H. Stapelfeldt, J. Chem. Phys. **111**, 7774 (1999).

[10] Y. Fujimura and H. Sakai, *Electronic and Nuclear Dynamics in Molecular Systems* (World Scientific, Singapore, 2011), Chap. 4, where some representative applications are reviewed.

[11] B. Friedrich and D. Herschbach, J. Chem. Phys. **111**, 6157 (1999).

[12] B. Friedrich and D. Herschbach, J. Phys. Chem. A **103**, 10280 (1999).

[13] H. Sakai, S. Minemoto, H. Nanjo, H. Tanji, and T. Suzuki, Phys. Rev. Lett. **90**, 083001 (2003).

[14] S. Minemoto, H. Nanjo, H. Tanji, T. Suzuki, and H. Sakai, J. Chem. Phys. **118**, 4052 (2003).

[15] H. Tanji, S. Minemoto, and H. Sakai, Phys. Rev. A **72**, 063401 (2005).

[16] Y. Sugawara, A. Goban, S. Minemoto, and H. Sakai, Phys. Rev. A **77**, 031403 (2008).

[17] A. Goban, S. Minemoto, and H. Sakai, Phys. Rev. Lett. **101**, 013001 (2008).

[18] L. Holmegaard, J. H. Nielsen, I. Nevo, H. Stapelfeldt, F. Filsinger, J. Küpper, and G. Meijer, Phys. Rev. Lett. **102**, 023001 (2009).

[19] O. Ghafur, A. Rouzée, A. Gijsbertsen, W. K. Siu, S. Stolte, and M. J. Vrakking, Nat. Phys. **5**, 289 (2009).

[20] J. H. Mun, D. Takei, S. Minemoto, and H. Sakai, Phys. Rev. A **89**, 051402 (2014).

[21] D. Takei, J. H. Mun, S. Minemoto, and H. Sakai, Phys. Rev. A **94**, 013401 (2016).

[22] T. Kanai and H. Sakai, J. Chem. Phys. **115**, 5492 (2001).

[23] K. Oda, M. Hita, S. Minemoto, and H. Sakai, Phys. Rev. Lett. **104**, 213901 (2010).

[24] M. Muramatsu, M. Hita, S. Minemoto, and H. Sakai, Phys. Rev. A **79**, 011403 (2009).

[25] S. De, I. Znakovskaya, D. Ray, F. Anis, N. G. Johnson, I. A. Bocharova, M. Magrakvelidze, B. D. Esry, C. L. Cocke, I. V. Litvinyuk, and M. F. Kling, Phys. Rev. Lett. **103**, 153002 (2009), see Note added in Ref. [23].

[26] E. Frumker, C. Hebeisen, N. Kajumba, J. Bertrand, H. J. Wörner, M. Spanner, D. Villeneuve, A. Naumov, and P. Corkum, Phys. Rev. Lett. **109**, 113901 (2012).

[27] P. M. Kraus, D. Baykusheva, and H. J. Wörner, Phys. Rev. Lett. **113**, 023001 (2014).

[28] See Supplemental Material at http://link.aps.org/supplemental/10.1103/PhysRevA.99.043420 for the explanations of the Wigner D-matrix and some fundamentals relevant to our article.

[29] R. I. Keir and G. L. Ritchie, Chem. Phys. Lett. **290**, 409 (1998).

[30] D. L. Mills, *Nonlinear Optics: Basic Concepts*, 2nd ed. (Springer, Berlin, 1998), p. 47.

[31] Each dot in the inset of Fig. 3 is plotted based on the following procedure: A state in the thermal ensemble according to the Boltzmann distribution at 1 K is selected by the Malkov chain Monte Carlo method. The Hamiltonian is stable and set as the intensities of the two wavelengths are both $3.0 \times 10^{12}\,\mathrm{W/cm^2}$. Then a point in the unit 3-sphere, which has a one-to-one correspondence with an element in SU(2), is randomly picked up. The probability density on the point is calculated. If it is larger than a uniform random number in [0,1], one of a projected leg of the molecule is plotted. If not, nothing is plotted. This process was repeated until 1000 points are plotted.

[32] K. Mizuse, K. Kitano, H. Hasegawa, and Y. Ohshima, Sci. Adv. **1**, e1400185 (2015).

[33] X. Liu, X. Zhu, L. Li, Y. Li, Q. Zhang, P. Lan, and P. Lu, Phys. Rev. A **94**, 033410 (2016).